

Dislocation Modelling of the 1997-2009 High-Precision Global Positioning System Displacements in Darjiling-Sikkim Himalaya, India

Kutubuddin Ansari, Malay Mukul, Sridevi Jade

Abstract—We used high-precision Global Positioning System (GPS) to geodetically constrain the motion of stations in the Darjiling-Sikkim Himalayan (DSH) wedge and examine the deformation at the Indian-Tibetan plate boundary using IGS (International GPS Service) fiducial stations. High-precision GPS based displacement and velocity field was measured in the DSH between 1997 and 2009. To obtain additional insight north of the Indo-Tibetan border and in the Darjiling-Sikkim-Tibet (DaSiT) wedge, published velocities from four stations J037, XIGA, J029 and YADO were also included in the analysis. India-fixed velocities or the back-slip was computed relative to the pole of rotation of the Indian Plate (Latitude $52.97 \pm 0.22^\circ$, Longitude $-0.30 \pm 3.76^\circ$, and Angular Velocity $0.500 \pm 0.008^\circ/\text{Myr}$) in the DaSiT wedge. Dislocation modelling was carried out with the back-slip to model the best possible solution of a finite rectangular dislocation or the causative fault based on dislocation theory that produced the observed back-slip using a forward modelling approach. To find the best possible solution, three different models were attempted. First, slip along a single thrust fault, then two thrust faults and in finally, three thrust faults were modelled to simulate the back-slip in the DaSiT wedge. The three-fault case bests the measured displacements and is taken as the best possible solution.

Keywords—Global Positioning System, Darjiling-Sikkim Himalaya, Dislocation modelling.

I. INTRODUCTION

THE motion of Indian plate occurs on a near-spherical Earth. It is, therefore, characterized by an Euler pole whose average angular velocity in ITRF 2005 reference frame is $0.500 \pm 0.008^\circ/\text{Myr}$ [1]. GPS measurements allow the estimation of very short term deformation starting from the day a station is set-up and measured for the first time. In ITRF 2005 Bangalore (IISc; 43.179°N ; 77.017°E), Hyderabad (Hyd; 13.021°N ; 77.570°E) two IGS stations velocity represent Indian plate velocity, Lhasa (LHAS; 27.677°N ; 88.729°E) represent Tibetan plate velocity. The velocity of campaign mode stations shows motion of Darjiling-Sikkim area of Himalayan wedge causing shallow focused earthquakes. The question is how these earthquakes occur in the area. Here we have tried to model the possible faults that

are created due to the motion, causing seismicity in the area.

II. MATHEMATICAL MODELLING

The forward modelling used in this work is based on Coulomb 3.2 [2]. The Coulomb software is trying to find out if fault created then what will be the possible solution of this finite rectangular fault. Let us consider observed displacement is d and $G(m)$ is a function of finite rectangular fault parameters and s is slip. In case of strike slip fault slip will be strike slip and in case of thrust slip fault the slip will be thrust slip. If the fault is oblique then slip is given by:

$$S = s \cdot \cos \alpha + s \cdot \sin \alpha$$

where S is total slip and α is the rake of fault.

The relationship between dislocation field and the fault geometry can be given by [3]:

$$\begin{aligned} d &= sG(m) + \varepsilon \\ \varepsilon &= d - sG(m) \end{aligned}$$

where G is the Green function (length, width, depth, dip angle, and cartesian co-ordinate of GPS-station of the finite rectangular fault). Since rupture created by fault is not totally rectangular so ε represents an error.

For forward modeling we are trying to $\varepsilon \rightarrow 0$, then

$$\hat{d} = \hat{s}G(\hat{m})$$

where \hat{d} represents modeled displacement and \hat{m} is modeled parameters.

For convenience to get best fit solution we are considering poisson ration for continental crusts 0.25 [4].

Consider the case we have observed data d_1, d_2, \dots, d_n and the Green function of each observation data are G_1, G_2, \dots, G_n respectively, Then:

$$\begin{bmatrix} d_1 \\ d_2 \\ \vdots \\ d_n \end{bmatrix} = s \begin{bmatrix} G_1(m_1, m_2, \dots, m_p) \\ G_2(m_1, m_2, \dots, m_p) \\ \vdots \\ G_n(m_1, m_2, \dots, m_p) \end{bmatrix} + \begin{bmatrix} \varepsilon_1 \\ \varepsilon_2 \\ \vdots \\ \varepsilon_n \end{bmatrix}$$

where m_1, m_2, \dots, m_p are parameter (length, width, depth, dip angle) of the finite rectangular fault

Kutubuddin Ansari is with the Department of Earth Sciences, Indian Institute of Technology Bombay Mumbai-400076, India (Phone: (+91)9930837152; e-mail: kdansari@iitb.ac.in).

Malay Mukul is with the Department of Earth Sciences, Indian Institute of Technology Bombay Mumbai-400076, India (e-mail: malaymukul@iitb.ac.in).

Sridevi Jade is with the CSIR Fourth Paradigm Institute (Formerly CSIR CMMACS) Bangalore-560037, India (e-mail: sridevi@cmmacs.ernet.in).

$$\begin{bmatrix} \varepsilon_1 \\ \varepsilon_2 \\ \vdots \\ \varepsilon_n \end{bmatrix} = \begin{bmatrix} d_1 \\ d_1 \\ \vdots \\ d_n \end{bmatrix} - s \begin{bmatrix} G_1(m_1, m_2, \dots, m_p) \\ G_2(m_1, m_2, \dots, m_p) \\ \vdots \\ G_n(m_1, m_2, \dots, m_p) \end{bmatrix}$$

In case, errors are going to zero we will get modelled parameter of finite rectangular fault will be:

$$\begin{bmatrix} \hat{d}_1 \\ \hat{d}_2 \\ \vdots \\ \hat{d}_n \end{bmatrix} = \hat{s} \begin{bmatrix} G_1(\hat{m}_1, \hat{m}_2, \dots, \hat{m}_p) \\ G_2(\hat{m}_1, \hat{m}_2, \dots, \hat{m}_p) \\ \vdots \\ G_n(\hat{m}_1, \hat{m}_2, \dots, \hat{m}_p) \end{bmatrix}$$

These $\hat{m}_1, \hat{m}_2, \dots, \hat{m}_p$ give the best possible solution of a finite rectangular fault. If we have more than one strike and thrust faults then:

$$\begin{bmatrix} \hat{d}_1 \\ \hat{d}_2 \\ \vdots \\ \hat{d}_n \end{bmatrix} = \hat{s}_1^{str} \begin{bmatrix} G_{11}^{str}(\hat{m}_{s1}, \hat{m}_{s2}, \dots, \hat{m}_{sp}) \\ G_{12}^{str}(\hat{m}_{s1}, \hat{m}_{s2}, \dots, \hat{m}_{sp}) \\ \vdots \\ G_{1n}^{str}(\hat{m}_{s1}, \hat{m}_{s2}, \dots, \hat{m}_{sp}) \end{bmatrix} + \hat{s}_2^{str} \begin{bmatrix} G_{21}^{str}(\hat{m}_{s1}, \hat{m}_{s2}, \dots, \hat{m}_{sp}) \\ G_{22}^{str}(\hat{m}_{s1}, \hat{m}_{s2}, \dots, \hat{m}_{sp}) \\ \vdots \\ G_{2n}^{str}(\hat{m}_{s1}, \hat{m}_{s2}, \dots, \hat{m}_{sp}) \end{bmatrix} \\ + \dots + \hat{s}_x^{str} \begin{bmatrix} G_{x1}^{str}(\hat{m}_{s1}, \hat{m}_{s2}, \dots, \hat{m}_{sp}) \\ G_{x2}^{str}(\hat{m}_{s1}, \hat{m}_{s2}, \dots, \hat{m}_{sp}) \\ \vdots \\ G_{xn}^{str}(\hat{m}_{s1}, \hat{m}_{s2}, \dots, \hat{m}_{sp}) \end{bmatrix} + \hat{s}_1^{thr} \begin{bmatrix} G_{11}^{thr}(\hat{m}_{d1}, \hat{m}_{d2}, \dots, \hat{m}_{dp}) \\ G_{12}^{thr}(\hat{m}_{d1}, \hat{m}_{d2}, \dots, \hat{m}_{dp}) \\ \vdots \\ G_{1n}^{thr}(\hat{m}_{d1}, \hat{m}_{d2}, \dots, \hat{m}_{dp}) \end{bmatrix} \\ + \hat{s}_2^{thr} \begin{bmatrix} G_{21}^{thr}(\hat{m}_{d1}, \hat{m}_{d2}, \dots, \hat{m}_{dp}) \\ G_{22}^{thr}(\hat{m}_{d1}, \hat{m}_{d2}, \dots, \hat{m}_{dp}) \\ \vdots \\ G_{2n}^{thr}(\hat{m}_{d1}, \hat{m}_{d2}, \dots, \hat{m}_{dp}) \end{bmatrix} + \dots + \hat{s}_y^{thr} \begin{bmatrix} G_{y1}^{thr}(\hat{m}_{d1}, \hat{m}_{d2}, \dots, \hat{m}_{dp}) \\ G_{y2}^{thr}(\hat{m}_{d1}, \hat{m}_{d2}, \dots, \hat{m}_{dp}) \\ \vdots \\ G_{yn}^{thr}(\hat{m}_{d1}, \hat{m}_{d2}, \dots, \hat{m}_{dp}) \end{bmatrix}$$

The above result can be applied for Strike Slip and thrust fault. If we have to model an oblique fault the above equation will become:

$$\begin{bmatrix} \hat{d}_1 \\ \hat{d}_2 \\ \vdots \\ \hat{d}_n \end{bmatrix} = \hat{s} \cos \alpha \begin{bmatrix} G_1^{str}(\hat{m}_{s1}, \hat{m}_{s2}, \dots, \hat{m}_{sp}) \\ G_2^{str}(\hat{m}_{s1}, \hat{m}_{s2}, \dots, \hat{m}_{sp}) \\ \vdots \\ G_n^{str}(\hat{m}_{s1}, \hat{m}_{s2}, \dots, \hat{m}_{sp}) \end{bmatrix} + \hat{s} \sin \alpha \begin{bmatrix} G_1^{thr}(\hat{m}_{d1}, \hat{m}_{d2}, \dots, \hat{m}_{dp}) \\ G_2^{thr}(\hat{m}_{d1}, \hat{m}_{d2}, \dots, \hat{m}_{dp}) \\ \vdots \\ G_n^{thr}(\hat{m}_{d1}, \hat{m}_{d2}, \dots, \hat{m}_{dp}) \end{bmatrix}$$

III. RESULTS AND DISCUSSION

The east component of the measured back-slip field is low and does not show much variation (Fig. 1). Therefore, dislocation modelling was carried out only with the north component of the back-slip to model the causative fault(s) that could have produced the observed back-slip surface displacements (Fig. 2). The dislocation modelling of the back-slip in the DSH reveals several important insights. First, a single dislocation was unable to effectively simulate the back-slip velocity field in the DSH wedge (Fig. 3). Therefore, the standard methodology of attributing a single dislocation to explain strain accumulation in the Himalaya may be too simplistic. We have not investigated the possibility of including an additional transverse strike-slip fault to further fine tune the velocity modelled at stations LAVA and KYON (Fig. 2).

In the three-dislocation model that best simulated the measured back-slip velocity field (Fig. 3), a slip of around 20 mm/yr (Table I) was postulated on Fault 1 suggesting that, this is the major out-of-sequence fault in the DSH at present. This is followed by LHD activity associated with Fault 2 where a slip of around 8 mm/yr (Table I) is postulated by the model. Finally, a slip of 1 mm/yr (Table I) is postulated by the model on Fault 3 close to the Himalayan mountain front. The seismicity in the DSH is largely confined to the frontal part of the wedge which indicates that the slip along faults 2 & 3 is seismic whereas slip along fault 1 is a seismic creep and could be related to an extruding ductile channel [5].

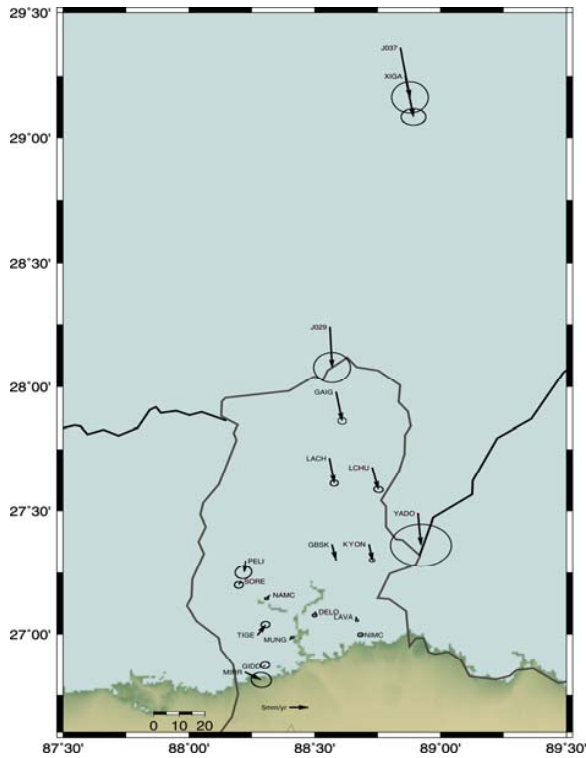


Fig. 1 India-fixed velocity field relative to the pole of rotation at Latitude $52.97 \pm 0.22^\circ$, Longitude $-0.30 \pm 3.76^\circ$, and Angular Velocity $0.500 \pm 0.008^\circ/\text{Myr}$ measured between 1997-2009 [6]

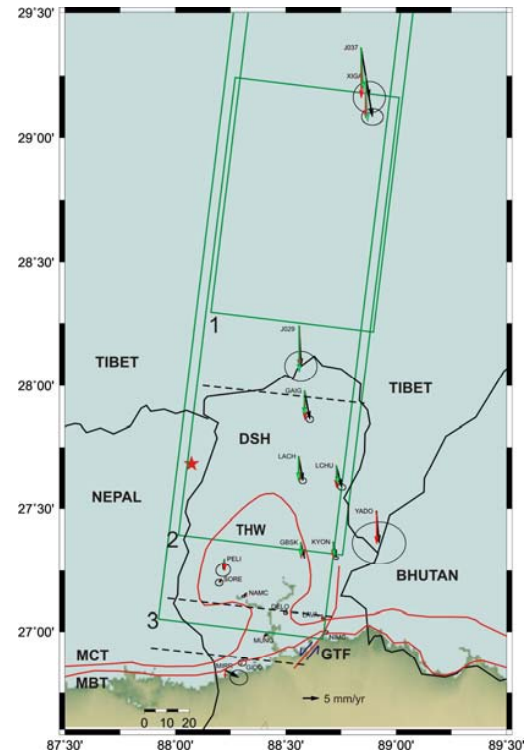


Fig. 2 Measured composite India-fixed velocities (black arrows), modelled (green) and measured (red) India-fixed north velocity relative to the pole of rotation at Latitude $52.97 \pm 0.22^\circ$, Longitude $-0.30 \pm 3.76^\circ$, and Angular Velocity $0.500 \pm 0.008^\circ/\text{Myr}$ [6] in DSH wedge is shown in the figure above. A three-dislocation model with parameters is used to try and simulate the measured velocity field. The red star is the epicenter of the 6.9 September 18, 2011 Sikkim earthquake and the black dashed lines are the projected surface traces of the three dislocations

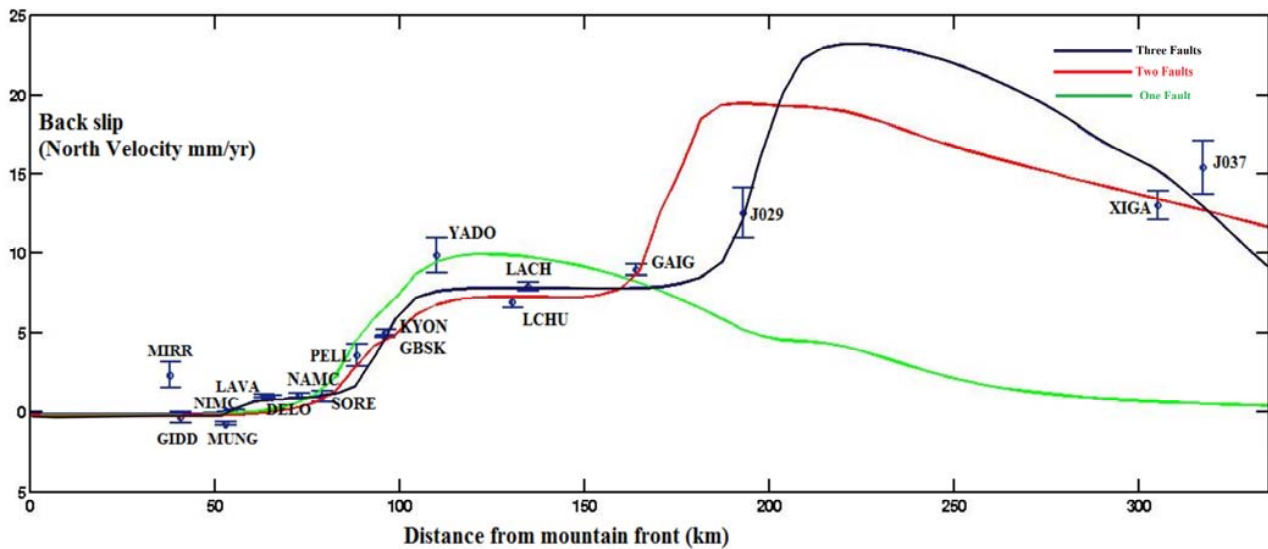


Fig. 3 Modelled back-slip velocity for one-dislocation (green-line), two-dislocation (red line) and three-dislocation (black line) along with the measured back-slip velocity at the GPS stations. The three-dislocation model simulates measured back-slip velocity field most closely

TABLE I
MODEL PARAMETERS

<i>Sr. No.</i>	<i>Length (Km)</i>	<i>Width (Km)</i>	<i>Bottom Depth(Km)</i>	<i>Top Depth(Km)</i>	<i>Dip Angle</i>	<i>Reverse Slip(mm)</i>	<i>Strike Slip(mm)</i>
1	73	149.16	16	3	5	20	6
2	73	200.70	16	2	4	8	1
3	73	286.71	21	1	4	1	0

IV. CONCLUSION

All the three dislocation models above (Fig. 3) simulate the frontal measured back-slip well. However, the one-dislocation model breaks down when we include velocities measured north of the Indo-Tibetan border [7]. A two-dislocation model is needed to simulate the back-slip in the entire wedge. However, a three-dislocation model simulates the measured back-slip in the entire Darjiling-Sikkim-Tibet Himalayan wedge best (Fig. 3).

ACKNOWLEDGEMENT

This work was funded by various grants from the Department of Science and Technology, Government of India to MM and SJ. KA acknowledges support from CSIR, through Junior and Senior Research Fellowships. Vinee Srivastava is thanked for drafting all the figures. Comments from two anonymous reviewers helped improve the manuscript.

REFERENCES

- [1] Jade, S., Bhattacharyya, A. K., Mukul, M., Jaganathan, S., Vijayan, M. S. M., Tiwari, R. P., Kumar, A., Kalita, S., Kumar, A., Krishna, A. P., Sahu, S. C., Murthy, M. V. R. L., Gupta, S. S. and Gaur, V. K. (2007). Estimates of interseismic deformation in Northeast India from GPS measurements, *Earth and Planetary Science Letters*, 263, 221–234.
- [2] Toda, S., Stein, R., Lin, J. and Sevilgen, V., “Coulomb 3.2 Graphic-rich deformation & Stress-change software for earthquake, tectonic and volcano research teaching”, 2010 (user guide).
- [3] P. Cervelli, M.H. Murray, P. Segall, Y. Aoki and T. Kato., “Estimating Source parameter from deformation data with an application to the March 1997 earthquake swarm of the Izu Peninsula, Japan” *Journal of Geophysical Research*, Vol. 106(10), 2001, p.11217-11237.
- [4] Nikolas I. Christensen, “Poisson ratio and crustal seismology”, *Journal of Geophysical Research*, Vol. 101(B2), 1996, p. 3139-3156.
- [5] Mukul, M., Jade, S., Ansari, K. and Matin, A., “Seismotectonic implications of strike-slip earthquakes in the Darjiling–Sikkim Himalaya” *Current Science*, vol. 106(2), 2014, p. 126-131.
- [6] Banerjee, P., Burgmann, R., Nagarajan, B. and Apel, E., “Intraplate deformation of the Indian subcontinent” *Geophysical Research Letters*, vol. 35, L18301, doi: 10.1029/2008GL035468, 2008.
- [7] Wang, Q., Zhang, P. Z., Freymueller, J. T., Bilham, R., Larson, K. M., Lai, X., You, X., Niu, Z., Wu, J., Li, Y., Liu, J., Yang, Z. and Chen, Q., “Present-day crustal deformation in China constrained by global positioning system measurements” *Science*, vol. 294, 2001, p. 574-577.